Nonlinear Ultrasound Modelling and Validation of Fatigue Damage

G.P. Malfense Fierro, F. Ciampa, D. Ginzburg, E. Onder, M. Meo*

Material Research Centre, Department of Mechanical Engineering, University of Bath, Bath, BA2 7AY, UK

*Corresponding author: m.meo@bath.ac.uk

Abstract

Nonlinear ultrasound techniques have shown greater sensitivity to microcracks and they can be used to detect structural damages at their early stages. However, there is still a lack of numerical models available in commercial finite element analysis (FEA) tools that are able to simulate the interaction of elastic waves with the materials nonlinear behaviour. In this study, a nonlinear constitutive material model was developed to predict the structural response under continuous harmonic excitation of a fatigued isotropic sample that showed anharmonic effects. Particularly, by means of Landau's theory and Kelvin tensorial representation, this model provided an understanding of the elastic nonlinear phenomena such as the second harmonic generation in three-dimensional solid media. The numerical scheme was implemented and evaluated using a commercially available FEA software LS-DYNA, and it showed a good numerical characterisation of the second harmonic amplitude generated by the damaged region known as the nonlinear response area (NRA). Since this process requires only the experimental second-order nonlinear parameter and rough damage size estimation as an input, it does not need any baseline testing with the undamaged structure or any dynamic modelling of the fatigue crack growth. To validate this numerical model, the second-order nonlinear parameter was experimentally evaluated at various points over the fatigue life of an Aluminium (AA6082-T6) coupon and the crack propagation was measured using an optical microscope. A good correlation was achieved between the experimental set-up and the nonlinear constitutive model.

Keywords: Nondestructive Evaluation Techniques, Nonlinear Ultrasound, Finite Element Method, Fatigue Life.

Introduction

Ultrasound testing can be broken into two main fields: (i) linear acoustic/ultrasonic methods and (ii) nonlinear ultrasound methods. Linear methods analyse wave speed changes and amplitude variations due to reflections of waves caused by structural damages. These techniques work satisfactory in the presence of a significant impedance contrast. However, when micro-damages are present in the form of nonlinear elastic zones rather than a heterogeneous elastic medium, these methods have difficulties in determining the extent of the defect [1, 2]. To overcome this limitation, a greater sensitivity to damage presence is offered by a promising new class of Non-Destructive Evaluation (NDT) techniques and Structural Health Monitoring (SHM) systems based on the evaluation of material nonlinear elastic behaviour. These methods have proved their effectiveness by detecting early signs of material degradation long before changes of the linear acoustic properties become prominent [3-5]. Consequently, a deeper understanding of nonlinear behaviour of solids along with their microscopic structure and dynamics is essential to evaluate the integrity of the medium, hence the development of a nonlinear ultrasound model to predict damage. Ordinary materials such as aluminium, composites and numerous others, exhibit *anharmonic effects* that can be explained by the classical nonlinear theory of Landau [6], known as Classical Nonlinear Elasticity (CNE). Nonlinear elastic effects of damaged materials can be assessed with nonlinear elastic wave spectroscopy (NEWS) [4, 5, 7, 8] and phase symmetry analysis (PSA) techniques [9] which explicitly interrogate the material nonlinear elastic behaviour and its effect on wave propagation caused by the presence of defects.

The focus of this work was to develop a material constitutive model that would accurately predict the nonlinear ultrasound effects (modulation, sub-harmonic, and further harmonic production) produced by damaged or cracked regions of a material. In order to investigate whether the nonlinear response of a material incorporating a crack could be simulated by means of numerical analysis, various methodologies using finite element modelling (FEM) techniques for damage representation were

investigated [10, 11]. For this purpose, the commercial explicit finite element analysis (FEA) software LS-DYNA 971 was used.

Experimental tests were performed on the aluminium dogbone at various points during its fatigue life to determine the nonlinear behaviour caused by crack propagation. It has been shown in many studies [3, 12, 13] that the production of further harmonics (at twice and three times the fundamental frequency) can be directly related to damage or the increase in damage. It has also been shown that the second order nonlinearity parameter β, determined by relating the fundamental frequency and the nonlinear second harmonic responses, increases as crack propagation increases over the fatigue life of a component [14]. The generation of such harmonics can be attributed to the 'clapping or rubbing' of a damaged region, which are excited by small stresses generated by a waves propagation through the medium. The material constitutive model developed was used to determine the generation of these further harmonics by attributing nonlinear behaviour to a nonlinear response area (NRA) within a FEA model. The elements which would behave in such a nonlinear manner would be representative of a cracked or damaged region. By propagating a specific frequency through the modelled medium, elements that exhibited the nonlinear behaviour generated further harmonics.

The experimental design and setup was used to validate: (i) the further harmonic generation, (ii) the magnitude of β (second order nonlinearity parameter), (iii) the crack size, and (iv) the fatigue life percentage of the component. Using the constitutive model and the experimental β determined it was possible to evaluate the generation of further harmonic production in the modelled solution. The modelled magnitude of the second harmonic was compared with the experimental data to assess its accuracy. By increasing the size of the NRA it was possible to: (i) evaluate the increase of the modelled second harmonic, (ii) determine if the increase in harmonic generation corresponded to experimental results, and (iii) confirm that the implemented NRA's responded effectively to single frequency excitation in a comparable manner as actual damaged regions (in this case a propagating crack).

The results showed that the modelling of the nonlinear elastic effect using the determined model correlated well to experimental results. Therefore the model developed provides the first step in potential FEA methods which will allow: (i) the incorporation of nonlinear ultrasound effects in

modeling, (ii) assessment of the generation and dispersion of nonlinearities due to damage in complex structures, (iii) the generation of more complex and realistic models, and (iv) estimation of residual fatigue life of components without baseline tests.

Nonlinear Constitutive Material Model

Linear stress-strain relationship defined in Hooke's law is usually inadequate to describe the nonlinear mechanical behaviour of solids with distributed damage (micro-cracks and micro voids) and with inelastic behaviour [15, 16]. Indeed, damaged materials such as aluminium, steel and composites that have atomic elasticity arising from atomic-level forces between atoms and molecules, exhibit classical nonlinear (also known as *anharmonic*) effects which can be described by the nonlinear elastic theory of Landau [17]. Particularly, the expression of the nonlinear elastic modulus K_C can be obtained through a one-dimensional (1D) power law expansion of the stress with respect to the strain ε:

$$K_C = K_0\left(1 + \beta\varepsilon + \delta\varepsilon^2 + \cdots\right) \tag{1}$$

where K_0 is the linear elastic modulus, β and δ are classical second order and third order nonlinear coefficients. In the up-scaling from microscopic to mesoscopic level (with dimensions of nearly 1-10 mm), both the linear elastic modulus and the nonlinear parameters can be assumed as constants within a solid element. Hence, Eq. (1) can be used to predict the nonlinear response of the material. However, for most solids the first nonlinear term β is sufficient to describe the nonlinear response. This coefficient can be experimentally obtained from the measurement of the second harmonic amplitude generated from a single pure tone input [18]. Since Eq. (1) represents a scalar model it cannot be used to investigate the three-dimensional (3D) material response of a cracked sample when different types of waves (bulk waves, guided waves, etc…) are applied.

Hence, to overcome this limitation, Kelvin notation was used to extend the standard Voigt stress-strain formulation in a tensorial equivalent form for the 3D Cartesian space [19]. Indeed, by introducing Kelvin representation, the Voigt stress-strain relationship for a homogeneous elastic medium becomes:

$$\tilde{\boldsymbol{\sigma}} = \tilde{\mathbf{K}}\tilde{\boldsymbol{\varepsilon}} \tag{2}$$

where the new components of the 6D stress and strain vectors are:

$$\begin{aligned}\widetilde{\boldsymbol{\sigma}} &= \left(\sigma_{11},\sigma_{22},\sigma_{33},\sqrt{2}\sigma_{12},\sqrt{2}\sigma_{13},\sqrt{2}\sigma_{23}\right)^T \\ \widetilde{\boldsymbol{\varepsilon}} &= \left(\varepsilon_{11},\varepsilon_{22},\varepsilon_{33},\sqrt{2}\varepsilon_{12},\sqrt{2}\varepsilon_{13},\sqrt{2}\varepsilon_{23}\right)^T\end{aligned} \tag{3}$$

and $\widetilde{\mathbf{K}}$ is the new six by six stiffness matrix defined by:

$$\widetilde{\mathbf{K}} = \mathbf{TKT} \text{ with } \mathbf{T} = \begin{bmatrix} \mathbf{I} & 0 \\ 0 & \sqrt{2}\mathbf{I} \end{bmatrix} \tag{4}$$

where $\mathbf{K}$ is the stiffness matrix in Voigt formulation. The symmetric matrix $\widetilde{\mathbf{K}}$ can be shown to represent the components of a second-rank tensor in the 6D space [20]. In accordance with Ciampa et al. [21, 22], the aim of this approach consists of determining the eigenmoduli $\boldsymbol{\Lambda}$ and the associated eigentensors $\widetilde{\boldsymbol{\varepsilon}}$ of Eq. (2) in order to form an ortho-normalized basis for the stress and strain tensors of the second rank. In this manner, these tensors can be decomposed with respect to this basis in the six-dimensional (6D) space. In other words, we seek for the eigenvalues $\boldsymbol{\Lambda}$ (known as *Kelvin moduli*) that satisfy the following equation:

$$\left(\widetilde{\mathbf{K}} - \boldsymbol{\Lambda}\mathbf{I}\right)\widetilde{\boldsymbol{\varepsilon}} = 0\,. \tag{5}$$

Since the 6D linear transformation $\widetilde{\mathbf{K}}$ is assumed to be symmetric and positive definite, there will be a maximum of six positive eigenelastic constants Λ_i $(i = 1,\ldots,6)$ associated to Eq. (5). In addition to the six values of $\boldsymbol{\Lambda}$, also six values of $\widetilde{\boldsymbol{\varepsilon}}$ will be associated to the problem (5), which are denoted by the vector $\widetilde{\boldsymbol{\varepsilon}}^{(i)}$ in the 6D space. The stresses $\widetilde{\boldsymbol{\sigma}}^{(i)}$ obtained by multiplying $\widetilde{\boldsymbol{\varepsilon}}^{(i)}$ by the eigenvalues Λ_i are called the stress eigentensors. Therefore, a Cartesian basis in the 6D space can be constructed from the normalized strain eigentensors, denoted by $\widetilde{\mathbf{N}}$:

$$\widetilde{\boldsymbol{\varepsilon}} = \widetilde{\mathbf{N}}\left|\widetilde{\boldsymbol{\varepsilon}}\right|; \quad \left|\widetilde{\boldsymbol{\varepsilon}}\right|^2 = \widetilde{\boldsymbol{\varepsilon}} \cdot \widetilde{\boldsymbol{\varepsilon}}; \quad \widetilde{\mathbf{N}} \cdot \widetilde{\mathbf{N}} = 1\,. \tag{6}$$

Hence, the stress eigentensors can be written in terms of the normalized strain eigentensors using Eqs. (2), (5) and (6) as:

$$\widetilde{\boldsymbol{\sigma}}^{(i)} = \Lambda_i \widetilde{\boldsymbol{\varepsilon}}^{(i)}\,. \tag{7}$$

With respect to the 6D space, $\widetilde{\boldsymbol{\sigma}}$, $\widetilde{\boldsymbol{\varepsilon}}$ and $\widetilde{\mathbf{K}}$ have the following representation:

$$\begin{aligned}\widetilde{\boldsymbol{\sigma}} &= \sum_{i=1}^{6}\Lambda_i\widetilde{\boldsymbol{\varepsilon}}^{(i)} = \sum_{i=1}^{6}\Lambda_i\left|\widetilde{\boldsymbol{\varepsilon}}^{(i)}\right|\widetilde{\mathbf{N}}^{(i)} \\ \widetilde{\boldsymbol{\varepsilon}} &= \sum_{i=1}^{6}\widetilde{\boldsymbol{\varepsilon}}^{(i)} = \sum_{i=1}^{6}\left|\widetilde{\boldsymbol{\varepsilon}}^{(i)}\right|\widetilde{\mathbf{N}}^{(i)}\end{aligned} \tag{8}$$

and:

$$\widetilde{\mathbf{K}} = \sum_{i=1}^{6}\Lambda_i\widetilde{\mathbf{N}}^{(i)}\otimes\widetilde{\mathbf{N}}^{(i)} \tag{9}$$

where $\otimes$ indicated the tensor or dyadic product. The projection of the strain state given by Eq. (3) along the eigenvectors obtained using Eq. (8) defines the eigenstrain vector $\widetilde{\varepsilon}_i$. Thereby, the total elastic modulus due to nonlinear material behaviour defined in Eq. (1) becomes:

$$\widetilde{K}_{TOT,i} = \Lambda_i\left(1+\beta\widetilde{\varepsilon}_i+\delta\widetilde{\varepsilon}_i^{2}+\cdots\right) \tag{10}$$

Once the total elastic modulus $\widetilde{K}_{TOT,i}$ ($i=1,\ldots,6$) is obtained, according to Eqs. (10) and (9), the 6 x 6 nonlinear stiffness matrix $\mathbf{K}_{TOT}$ can be then transformed from Kelvin to Voigt notation and it can be used for the implementation of the explicit FE numerical method at each individual time step.

Nonlinear Finite Element Model

The application of explicit FE analysis in wave propagation problems allows computing the nodal forces and displacements without recourse to a factorisation of the global stiffness matrix in a step-by-step solution. Let us consider a 3D solid domain Ω with boundary Γ discretized with three-dimensional elements. The weak form of the equilibrium equations for the continuum Ω can be derived from the displacement variational principle as follows [23]:

$$\mathbf{M}\ddot{\mathbf{u}} = \mathbf{F}^{ext} - \mathbf{F}^{\text{int}} \tag{11}$$

where the dots superscript denotes a second time derivative operation of the global displacement vector $\mathbf{u}$ and the external nodal forces vector $\mathbf{F}^{ext}$, the internal nodal forces vector $\mathbf{F}^{\text{int}}$ and the (lumped) diagonal mass matrix $\mathbf{M}$ are:

$$\mathbf{F}^{\text{int}} = \sum_{e=1}^{n_{el}}\mathbf{L}^{(e)T}\mathbf{C}^{(e)}\mathbf{L}^{(e)}\mathbf{u} \tag{12a}$$

$$\mathbf{F}^{ext} = \sum_{e=1}^{n_{el}} \mathbf{L}^{(e)T} \left[\int_{\Gamma^{(e)}} \mathbf{\Phi}^T \mathbf{t} d\Gamma + \int_{\Omega^{(e)}} \mathbf{\Phi}^T \mathbf{b}\, d\Omega \right] \tag{12b}$$

$$\mathbf{M} = \sum_{e=1}^{n_{el}} \mathbf{L}^{(e)T} \mathbf{m}^{(e)} \mathbf{L}^{(e)} \tag{12c}$$

where $\mathbf{L}^{(e)}$ is the Boolean connectivity matrix that gather the nodal displacement $\mathbf{d}^{(e)}$ of each element e to the global one over the entire domain Ω, n_{el} is the total number of elements, $\Omega^{(e)}$ and $\Gamma^{(e)}$ are the element domain and its boundary, $\mathbf{\Phi}^T$ is the transpose of the shape function matrix, $\mathbf{t}$ and $\mathbf{b}$ are the surface traction and body (inertial) force of the element, respectively. The element stiffness matrix $\mathbf{C}^{(e)}$ in Eq. (12a) can be expressed in terms of the nonlinear stiffness matrix $\mathbf{K}_{TOT}$ as follows [24]:

$$\mathbf{C}^{(e)} = \int_{\Omega^{(e)}} \mathbf{B}^T \mathbf{K}_{TOT} \mathbf{B}\, d\Omega \tag{13}$$

whilst the element mass matrix in Eq. (12c) is:

$$\mathbf{m}^{(e)} = \int_{\Omega^{(e)}} \rho \mathbf{\Phi}^T \mathbf{\Phi} d\Omega . \tag{14}$$

Finally, the strain nodal displacement matrix is defined by:

$$\boldsymbol{\varepsilon} = \mathbf{B}\mathbf{L}^{(e)}\mathbf{u} \tag{15}$$

The global displacement at the instant of time k+1 using the central difference method is given by:

$$\mathbf{u}_{k+1} = \Delta t^2 \mathbf{M}^{-1} \left(\mathbf{F}_k^{ext} - \mathbf{F}_k^{\text{int}} \right) + 2\mathbf{u}_k - \mathbf{u}_{k-1} . \tag{16}$$

where k=0, 1, 2, … corresponds to times $t = 0$, $t = T$, $t = 2T$, …, and T is the time increment. To guarantee numerical stability to the method, the time increment used for the simulation satisfy the following condition [25]:

$$\begin{aligned} & T < T_{cr} \\ & T_{cr} = \frac{1}{\pi} \frac{1}{f_{\max}} \end{aligned} \tag{17}$$

where f_{max} is the largest natural frequency of the system. The numerical scheme defined by Eq. (16) can be used by those elements that present either linear or nonlinear features. Whilst in the former case, the nonlinear elastic moduli are zero, in the nonlinear case the nonlinear stiffness matrix of the

element has to be constantly updated at each time step due to the amplitude dependence with the material constants.

FE Model and Specimen Dimensions

Crack Representation Modelling

One way to represent a crack inside a specimen is to attempt to accurately model the crack geometry and interfaces and to define appropriate contact conditions. However, this approach requires discretising the volume into very small finite elements due to the geometrical complexity of the crack interfaces; this inherently leads to distortion of the elements within the model [26].

An alternative method, which was adopted in this study, was to replace a damaged zone of the material with a user defined constitutive material model (UMAT) incorporating a classical nonlinearity representation theory in order to simulate a dynamic response of a test specimen with a crack. An isotropic elastic material was chosen as a base material model and no plastic deformations took place during the experiment.

Equations detailed in the previous section were incorporated into a user defined isotropic elastic material model with nonlinear parameters (*UMAT41*) using FORTRAN. This model was then linked with LS-DYNA solver to simulate a NRA of the test specimen. In the numerical procedure of the FE solver, strains and stresses are evaluated at every time step and for each element, which are in turn used at the next time step to update the internal forces.

Pre-Processing

Pre-processing of FEA problem involves creating the geometry, discretising the geometry into finite elements (i.e. meshing) and applying boundary conditions and forces. For this purpose, LS-PrePost 4.0 software tool was utilised.

The geometry was created using the dimensions of the test specimen Fig. (1). As the geometry is three-dimensional, it is required to be meshed using 3D solid elements. The mesh size was determined

by studying the numerical procedure used by LS-DYNA to calculate the time step size during the transient analysis. The solver uses Eq. (17) to determine the time step size during the simulation.

The time step was chosen to be the same value as the sampling rate required in order to achieve a good resolution of the sine wave signal applied to the specimen; the applied frequency was 100 kHz, for which the sampling rate was 10 MHz and therefore the time step size T was 1e-7 s. The speed of sound was calculated to be approximately 6000 m/s, and the following aluminium properties were used, i.e. E (Young's Modulus, GPa) = 70, ρ (Density, kg/mm^3) = 2.70e-6, ν (Poisson's Ratio) = 0.3. Having determined the time step and the speed of sound of the material, the element size was estimated to be 0.6 mm (i.e. length of a side of a cubic 3D solid element). Hence, the NRA of the specimen were meshed using 0.6 mm element size, whilst other features of the sample were meshed using element sizes up to 1.5 mm. *MAT001,* which is an isotropic elastic material, was used to represent the material of the specimen while the NRA was modelled using the user defined material *UMAT41*.

In the physical experiment, the specimen was simply supported at two ends. For the purpose of FE modelling, this was simulated by constraining the out-of-plane translational degrees of freedom (DOFs) of the nodes of the computational mesh of the test piece at two ends as shown in Fig. (2) using **BOUNDARY_SPC_SET* card within LS-PrePost.

The sine wave load was modelled by means of **LOAD_NODE_SET* card applying a sine load in out-of-plane direction on the nodes covering the area where the transducer was placed in the experimental setup. The **DEFINE_CURVE* card was used to supply a continuous sine wave load curve:

$$s(t) = A\sin(2\pi f_0 t) \tag{18}$$

where A is the amplitude (equal to 1kN) and f_0 is the excitation frequency.

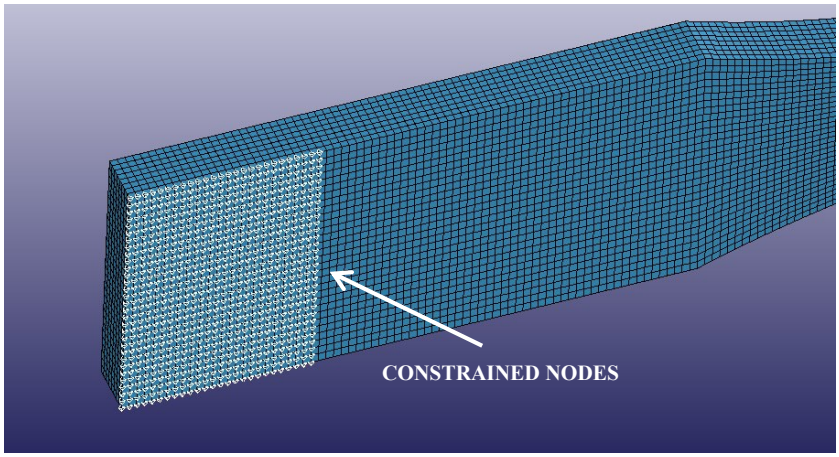

Figure 1: Selected nodes were constrained in out of plane direction in order to represent the experimental setup.

The final LS-DYNA deck contained approximately 72,000 3D solid elements modelled using *ELFORM=1* (i.e. constant stress element formulation) and nodal displacement histories were recorded at various locations throughout the specimen.

The simulation was run using a single precision SMP version of LS-DYNA on Intel Core i5 CPU utilising 4 cores clocked at 2.50GHz each. Wall clock computational time was 21 minutes.

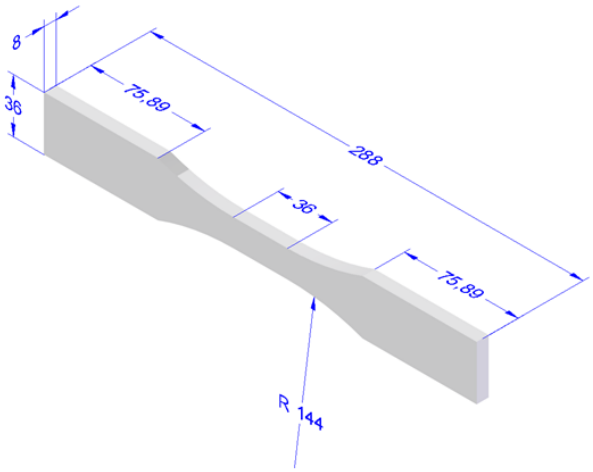

Figure 2: Dimensions of Dogbone specimen

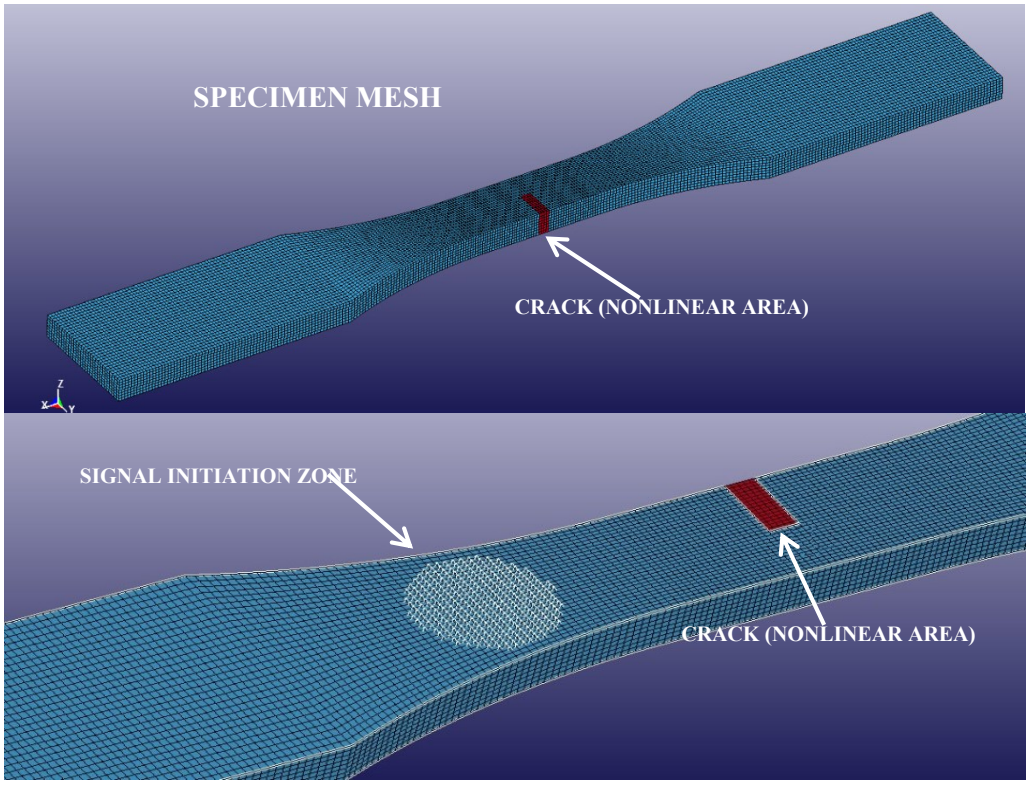

Figure 3: FEA model (elements, sensor and crack location)

Analytical Model

When exciting a structure using a single frequency excitation, the second-order (quadratic) nonlinear parameter (also known as β) generated by the presence of cracks or ruptures [27] can be defined as:

$$\beta = \frac{8A_2}{A_1^2 k^2 a_1} \tag{19}$$

where A_1 and A_2 are the amplitudes of the first and second harmonics of the recorded time domain waveforms, respectively, k is the wavenumber and a1 is the propagation distance. Eq. (19) was used to determine the experimental β, and was used within the constitutive model to determine the second harmonic ($2f_0$) produced by 'clapping/rubbing mechanisms' within the nonlinear response areas (NRA).

Experimental Setup

The experiment used a coupon that had been designed to allow for fatigue and crack growth. The samples geometry was representative of a classical dogbone for fatigue testing. The coupon was a high grade Aluminum 6082-T6, with a length of 288mm, thickness of 8mm, and breadth of 36mm. The design of the coupon ensured that: (i) high stress concentration areas existed, (ii) fatiguing of the sample focused on the initial crack region, and (iii) crack propagation occurred.

The piezoelectric sensor setup was determined by: (i) selecting the appropriate frequency, (ii) the use of broadband piezoelectric sensors, and (iii) assessing the production of harmonics at various piezoelectric sensor locations on the specimen. The piezoelectric sensors used (APC transducers) were glued in place and thus were attached to the coupon during the fatigue testing. This allowed evaluation of permanently installed transducers and evaluation of the proposed techniques in real-life conditions. The sending piezoelectric sensor was driven directly by an arbitrary waveform generator (TTi-TGA12104), and the receiving sensor was not amplified. The frequencies used were carefully selected. The arbitrary waveform generator was used to perform a sweep of the frequencies for various frequency ranges in order to determine the peaks of the second harmonic in the sample response. In this manner, the excitation frequency (f_0) used was 100 kHz. The specimen was tested at various intervals throughout its fatigue life using the excitation frequency in order to determine the nonlinear behaviour of the propagating crack.

The acquired signal, captured by Sensor 2 (Fig. 4), was recorded using an oscilloscope (Picoscope 4224) in the time domain and then converted into the frequency domain (using a Fast-Fourier transform) to evaluate the production of further harmonics (second harmonic). This data was then analyzed over the fatigue life of the specimen. The sampling frequency used was 20 MHz.

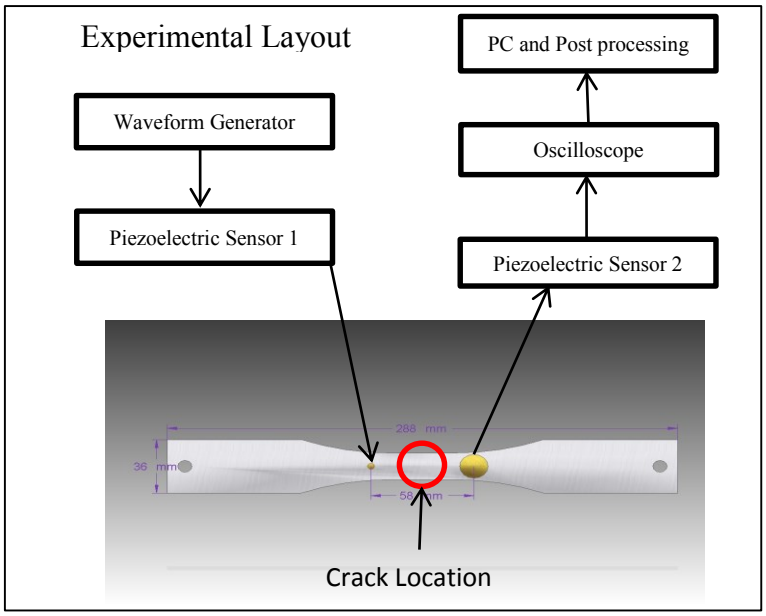

Figure 4: Experimental Layout

Numerical and Analytical Results

Crack Growth

The specimen was fatigued and tested using ultrasound at various points during its fatigue life. Figure 5 (below) shows the crack propagation length at 40000 cycles (90% of fatigue life) and the initial crack, measured using a microscope. The fatigue test was conducted using an Instron machine and was cyclic fatigued using sinusoidal tension with a stress ratio of 0.027 and amplitude of 18.5 kN. The material properties were carefully characterised before conducting the fatigue test to ensure crack propagation and specimen failure. The specimens showed consistent failure just above 40000 cycles. The consistency of the failure allowed accurate measurement of further harmonic production due to crack propagation.

Fatigue Life	0%, 25%, 32%, 40%, 87%, 99%
Number of Cycles	0, 10000, 13000, 16000, 35000, 40000
Stress Ratio ($\sigma_{min}/\sigma_{max}$)	0.027
Amplitude	18.5kN

Table I: Fatigue Characteristics

At each stage throughout the fatigue life of the specimen the second harmonic generation was assessed and compared with the fundamental frequencies amplitude in order to determine the second order nonlinearity parameter.

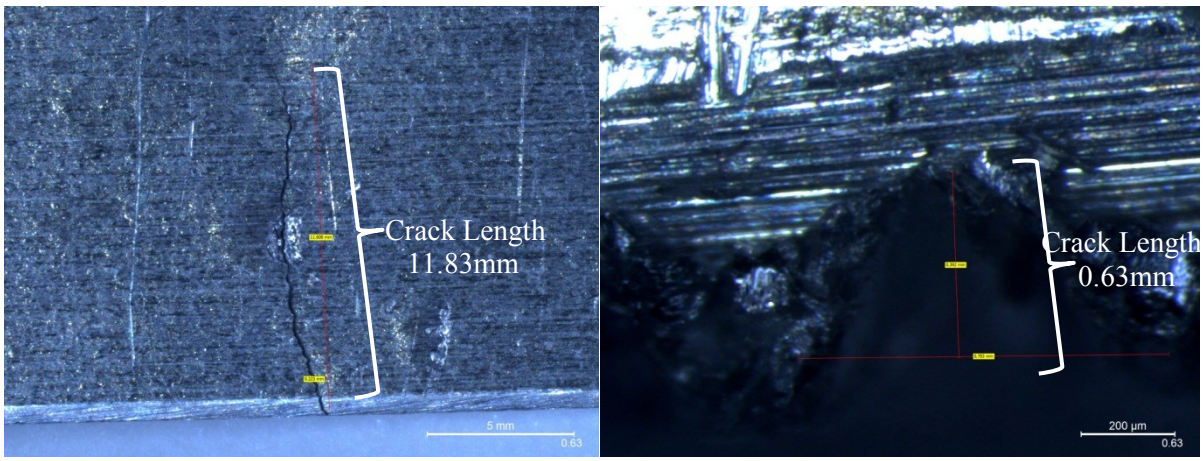

Figure 5: Crack propagation: 40000cycles (Left) and initial crack (Right)

Experimental and Numerical Results

The experimental β was used within the constitutive model in order to determine the level of the second harmonic. By applying the constitutive model and the experimental β to the NRA (areas of interest, representing damaged zones/crack propagation areas) it was possible to simulate the nonlinear material response.

During the post-processing step, the evolution of nodal displacements (recorded at various locations) through the specimen were plotted in the frequency domain by means of a Fast Fourier Transfer (FFT) using MATLAB software. These results (Figure 6) were initially computed for a stationary crack with dimensions of 5 x 5 x 2 mm in order to determine whether the computational model could be used to estimate the second harmonic level using the application of the material constitutive model. The specimen was then fatigue tested using the ultrasound methodology discussed earlier. The experimental results (Figure 6a) show the amplitude of the second harmonic at 200 kHz ($2f_0$) relative to the amplitude of the fundamental frequency (f_0) whilst the computational analysis (Figure 6b) results show a normalised frequency domain plot. Figure 6b, was determined by using the

experimental value of β within the numeric model in order to evaluate the second harmonic. The numeric model was able to estimate the level of the second harmonic with good accuracy.

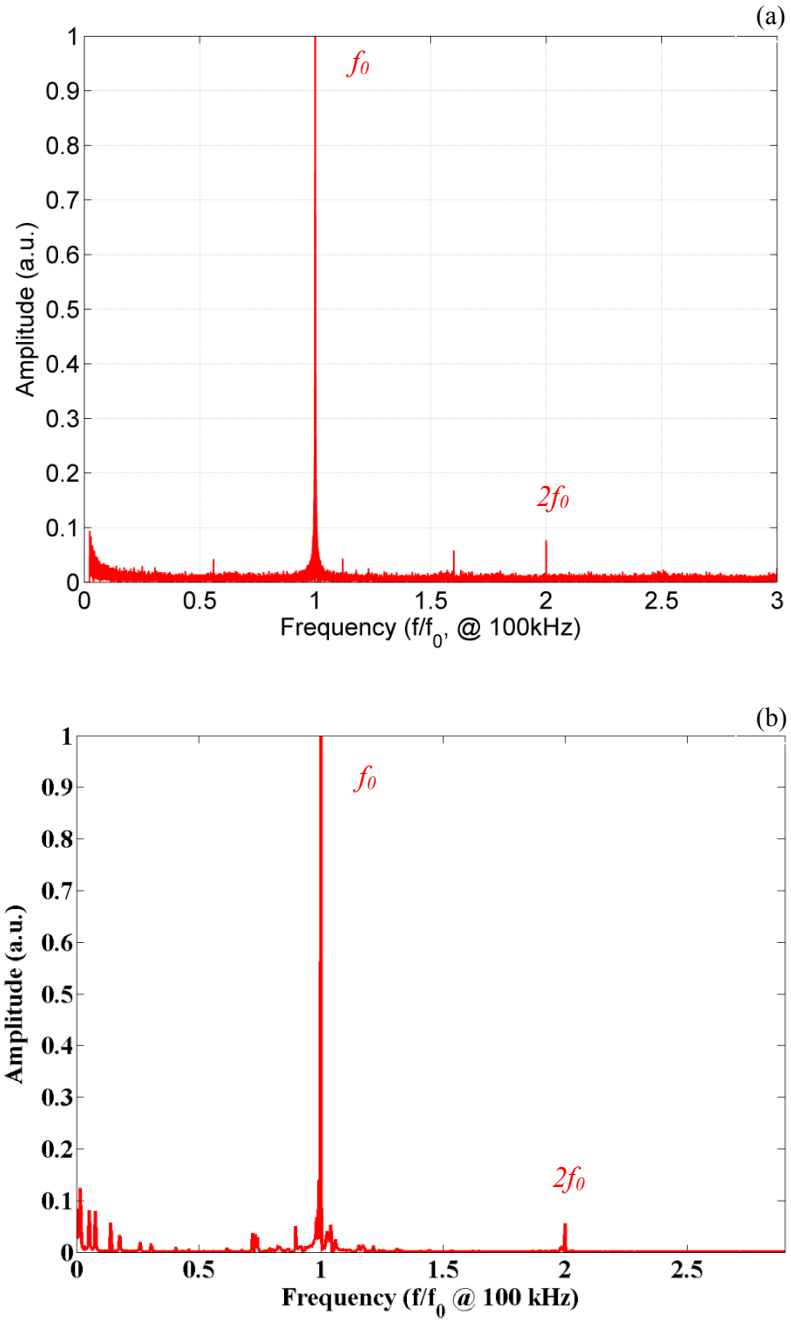

Figure 6: Normalised Experimental (a) vs. Normalised Numerical (b) Results (10000 cycles)

After the initial comparison between the constitutive model and the experimental results showed good correlation, the model was run with increasing NRA's to determine whether this increase would results in larger second harmonics.

Experimental results for the frequency tested confirmed a clear increase of the second order nonlinearity parameter (β) as fatigue life (and crack length) increased. The relationship between β and fatigue life showed that: (i) the increase in β was directly related to the fatigue life, resulting from a reduction in f_0 and increase in $2f_0$, (ii) the production of harmonics are directly related to the 'clapping/rubbing' mechanisms (i.e. cracks), as cracks increased in length so did the $2f_0$ generation, (iii) the growth of such mechanisms resulted in an increase in further harmonic production, and (iv) β can be used to estimate fatigue life.

In order to analyse the behaviour of the fundamental and second harmonics with crack propagation, images were taken using a microscope at each fatigue interval to determine the crack length. This allowed for visual confirmation that the second harmonic as well as β increased relative to the crack length. Taking into account that the production of the second harmonic allowed for the second order nonlinear parameter to be determined, a constitutive model that could predict $2f_0$ as crack length grows (increase in NRA) would provide valuable insight into the nonlinear, failure, and fatigue life mechanics of a component.

The model developed (Figure 7-dotted line) showed $2f_0$ increased as the NRA's grew representing the fatigue of the structure over its useful life. The increase in the numeric second harmonic showed good correlation with experimental results (solid line); as the NRA's were increased to represent larger cracks. It should be noted that element sizes were kept relatively large (in order to reduce computational times), but it is expected that greater accuracy could be achieved with finer meshes.

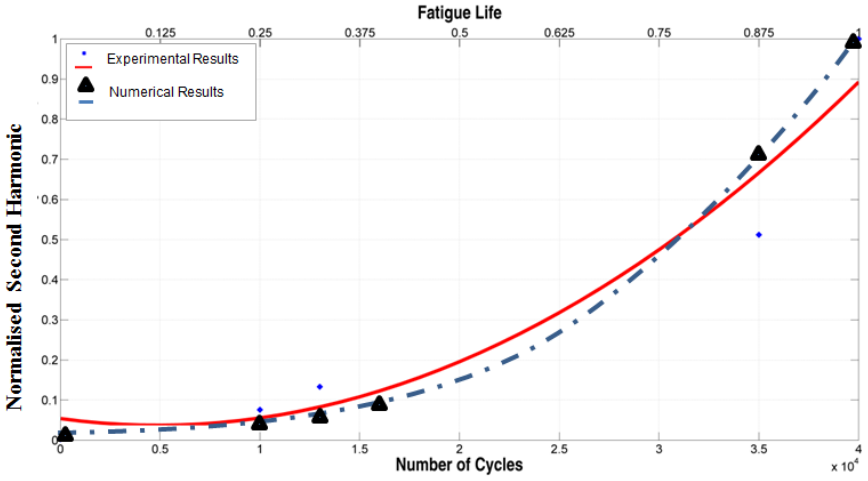

Figure 7: Normalised Second Harmonic vs. Fatigue life (Number of Cycles) at 100 kHz

The behaviour of NRA's using the developed constitutive model showed that: (i) the nonlinear behaviour which is directly correlated to the size of damaged regions can be modelled, (ii) element distortion is not an issue as the model developed does not require complicated design of cracks or other damage types, (iii) correlation between the model and experimental results were good, and (iv) it can be a useful tool to estimate the nonlinear behaviour of damaged regions at various stages over the fatigue life of a material.

A few considerations that should be taken into account regarding the developed model are: (i) the growth and propagation area of the crack were know, (ii) the specimen was designed to exhibit high stress concentration areas in known locations, (iii) fatiguing of the material was done accurately and used sinusoidal cycling, which would not be the case during the life cycle of a component, and (iv) simplicity of the shape of the specimen aids the developed model.

Conclusion

The work looked at developing a nonlinear constitutive material model that could predict the production of further harmonics which can be directly related to the extent of damage within a material. Nonlinear ultrasound methods have also been shown to be highly sensitive to damage compared with traditional methods such as linear ultrasound techniques. A material constitutive model was developed in LS-DYNA that could replicate and relate the production of further harmonics to a predefined nonlinear response area (NRA); this allowed for: (i) the estimation of the second harmonic after taking into account the experimental β value, and (ii) an estimation of damage progression related to the numeric generation of the second harmonic.

The experimental generation of harmonics and the increase of β as damaged increased showed that: (i) the results followed the expected theory that material damage results in further harmonics, (ii) the production of these further harmonics relative to the fundamental frequency increases with damage, and (iii) β can be used to estimate the fatigue life of the material.

The direct correlation between the generation of the second harmonic, damage, and the ability of the model to calculate the second harmonic showed that it can provide useful information about the

growth of damage within a component. The β derived experimentally was used within the model in order to assign nonlinear characteristics to known high stress regions or damaged regions, this allowed for the estimation of the second harmonic for various sized NRA's. Good correlation between the numerical prediction and experimental results were found for the prediction of the second harmonic.

The results of this work suggest that it is possible to generate FEA models based on nonlinear ultrasound theory and material models that would be able to estimate damage without the need of baseline tests of components. The robustness of the method relies on the comparison of the experimental and the numerical results, which showed good correlation.

References

[1] E.N., Janssen, K.V.D., Abeele, "Dual energy time reversed elastic wave propagation and nonlinear signal processing for localisation and depth-profiling of near-surface defects: A simulation study", *Ultrasonics* **51** (8), pp. 1036-1043, (2011)

[2] W., de Lima, M., Hamilton, "Finite-amplitude waves in isotropic elastic plates", *Journal of Sound and Vibration* **265** (4), pp. 819-839, (2003)

[3] K.-A., Van Den Abeele, P.A., Johnson, A., Sutin, "Nonlinear elastic wave spectroscopy (NEWS) techniques to discern material damage, part I: nonlinear wave modulation spectroscopy (NWMS)", *Research in nondestructive evaluation* **12** (1), pp. 17-30, (2000)

[4] M., Meo, G., Zumpano, "Nonlinear elastic wave spectroscopy identification of impact damage on a sandwich plate", *Composite Structures* **71** (3-4), pp. 469-474, (2005)

[5] G., Zumpano, M., Meo, "Damage localization using transient non-linear elastic wave spectroscopy on composite structures", *International Journal of Non-Linear Mechanics* **43** (3), pp. 217-230, (2008)

[6] L.-D., Landau, E.-M., Lifchits, A.-M., Kosevitch, L.-P., Pitaevski, J.-B., Sykes, W., Reid, L.-D., Landaou, L.-P., Pitaevski, Course of theoretical physics: Theory of elasticity, Butterworth-Heinemann, 1986.

[7] K. A., Van Den Abeele, P., Johnson, A., Sutin, "Nonlinear elastic wave spectroscopy (NEWS) techniques to discern material damage, part I: nonlinear wave modulation spectroscopy (NWMS)", *Res Nondestruct Eval* **12** (1), pp. 17-30, (2000)

[8] P., Johnson, "New wave in acoustic testing", *Mater. World* 7 (9), pp. 544-546, (1999)

[9] F., Ciampa, M., Meo, "Nonlinear elastic imaging using reciprocal time reversal and third order symmetry analysis", *The Journal of the Acoustical Society of America* 131, pp. 4316, (2012)

[10] S., Vanaverbeke, K., Van Den Abeele, "Two-dimensional modeling of wave propagation in materials with hysteretic nonlinearity", *The Journal of the Acoustical Society of America* 122, pp. 58, (2007)

[11] M., Scalerandi, V., Agostini, P.-P., Delsanto, K., Van Den Abeele, P.A., Johnson, "Local interaction simulation approach to modelling nonclassical, nonlinear elastic behavior in solids", *The Journal of the Acoustical Society of America* 113, pp. 3049, (2003)

[12] K.-Y., Jhang, "Nonlinear ultrasonic techniques for nondestructive assessment of micro damage in material: a review", *International journal of precision engineering and manufacturing* 10 (1), pp. 123-135, (2009)

[13] F., Amerini, M., Meo, "Structural health monitoring of bolted joints using linear and nonlinear acoustic/ultrasound methods", *Structural Health Monitoring* 10 (6), pp. 659-672, (2011)

[14] M., Amura, M., Meo, F., Amerini, "Baseline-free estimation of residual fatigue life using a third order acoustic nonlinear parameter", *The Journal of the Acoustical Society of America* 130, pp. 1829, (2011)

[15] L., Ostrovsky, P., Johnson, "Dynamic nonlinear elasticity in geomaterials", *Rivista del nuovo cimento* 24 (7), pp. 1-46, (2001)

[16] P.-A., Johnson, "The Universality of Nonclassical Nonlinearity (with application to Nondestructive Evaluation and Ultrasonics)", *Springer New York* Chap. 4 (49-69), (2006)

[17] L., Landau, E., Lifshitz, Pergamon Press, Oxford, UK, 1986.

[18] G., Zumpano, M., Meo, "A new damage detection technique based on wave propagation for rails", *International journal of solids and structures* 43 (5), pp. 1023-1046, (2006)

[19] K., Helbig, P.-N., Rasolofosaon, "A theoretical paradigm for describing hysteresis and nonlinear elasticity in arbitrary anisotropic rocks", *Anisotropy*, pp. 383-398, (2000)

[20] P., Theocaris, D., Sokolis, "Spectral decomposition of the compliance fourth-rank tensor for orthotropic materials", *Archive of Applied Mechanics* 70 (4), pp. 289-306, (2000)

[21] F., Ciampa, E., Barbieri, M., Meo, "Modelling of Multiscale Nonlinear Interaction of Elastic Waves with three dimenisonal Cracks", *J. Acoust. Soc. Am. 135 (4),* (2014) *doi: 10.1121/1.4868476*

[22] F., Ciampa, E., Onder, E., Barbieri, M., Meo, "Detection and Modelling of Nonlinear Elastic Response in Damage Composite Structures", *J. Nondestruct Eval.* (2014) *doi: 10.1007/s10921-014-0247-7*

[23] K.-J., Bathe, "Finite Element Procedures in Engineering Analysis", *Prentice-Hall Inc.*, (1982)

[24]. R.-D., Cook, D.-S, Malkus, M.E. Plesha, "Concepts and applications of finite element analysis", *third ed. John Wiley & Sons*, Hoboken, (1989)

[25] J., Donea, "Advanced Structural Dynamics", *Applied Science Publishers, Barking. Essex*, (1980)

[26] J., Sarrate Ramos, A., Huerta, "An improved algorithm to smooth graded quadrilateral meshes preserving the prescribed element size", Commun. Numer. Methods Eng. **17**(2):89–99 (2001)

[27] J.-H., Cantrell, "Fundamentals and applications of non-linear ultrasonic nondestructive evaluation", *Ultrasonic non-destructive evaluation* vol. 6 (Boca Raton (FL): CRC Press), pp. p.363-434, (2004)